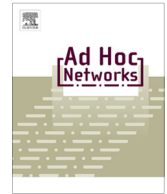




ELSEVIER

Contents lists available at ScienceDirect

Ad Hoc Networks

journal homepage: www.elsevier.com/locate/adhoc

Energy and spectrum-aware MAC protocol for perpetual wireless nanosensor networks in the Terahertz Band



Pu Wang^{a,*}, Josep Miquel Jornet^{b,1}, M.G. Abbas Malik^{c,1}, Nadine Akkari^{c,1}, Ian F. Akyildiz^{c,d,1}

^a Department of Electrical Engineering and Computer Science, Wichita State University, Wichita, KS 67260-0083, USA

^b Department of Electrical Engineering, University at Buffalo, The State University of New York, Buffalo, NY 14260, USA

^c Faculty of Computing and Information Technology, King Abdulaziz University, Jeddah, Saudi Arabia

^d Broadband Wireless Networking Laboratory, School of Electrical and Computer Engineering, Georgia Institute of Technology, Atlanta, GA30332, USA

ARTICLE INFO

Article history:

Received 12 June 2013

Accepted 16 July 2013

Available online 25 July 2013

Keywords:

Nanosensors

Nanonetworks

MAC

Terahertz Band

Energy harvesting

ABSTRACT

Wireless NanoSensor Networks (WNSNs), i.e., networks of nanoscale devices with unprecedented sensing capabilities, are the enabling technology of long-awaited applications such as advanced health monitoring systems or surveillance networks for chemical and biological attack prevention. The peculiarities of the Terahertz Band, which is the envisioned frequency band for communication among nano-devices, and the extreme energy limitations of nanosensors, which require the use of nanoscale energy harvesting systems, introduce major challenges in the design of MAC protocols for WNSNs. This paper aims to design energy and spectrum-aware MAC protocols for WNSNs with the objective to achieve fair, throughput and lifetime optimal channel access by jointly optimizing the energy harvesting and consumption processes in nanosensors. Towards this end, the critical packet transmission ratio (CTR) is derived, which is the maximum allowable ratio between the transmission time and the energy harvesting time, below which a nanosensor can harvest more energy than the consumed one, thus achieving perpetual data transmission. Based on the CTR, first, a novel symbol-compression scheduling algorithm, built on a recently proposed pulse-based physical layer technique, is introduced. The symbol-compression solution utilizes the unique elasticity of the inter-symbol spacing of the pulse-based physical layer to allow a large number of nanosensors to transmit their packets in parallel without inducing collisions. In addition, a packet-level timeline scheduling algorithm, built on a theoretical bandwidth-adaptive capacity-optimal physical layer, is proposed with an objective to achieve balanced single-user throughput with infinite network lifetime. The simulation results show that the proposed simple scheduling algorithms can enable nanosensors to transmit with extremely high speed perpetually without replacing the batteries.

© 2013 Elsevier B.V. All rights reserved.

1. Introduction

Nanotechnology is providing a new set of tools to the engineering community to create nanoscale components

with very specific functionalities, such as computing, data storing, sensing and actuation. Advanced nano-devices can be created by integrating several of these nano-components in a single entity. An early application of these nano-devices is in the field of nanosensing. Nanosensors take advantage of the unique properties of novel nanomaterials to detect new types of events at the nanoscale. WNSNs, i.e., networks of nanosensors, will enable advanced applications of nanotechnology in the biomedical field (e.g., intrabody health monitoring and drug delivery systems), in environmental research (e.g., agriculture plague and air

* Corresponding author.

E-mail addresses: pu.wang@wichita.edu (P. Wang), jmornet@buffalo.edu (J.M. Jornet), momalik@kau.edu.sa (M.G. Abbas Malik), nakkari@kau.edu.sa (N. Akkari), ian@ece.gatech.edu (I.F. Akyildiz).

¹ This paper was funded by King Abdulaziz University, under Grant No. (11-15-1432/HiCi). The authors, therefore, acknowledge technical and financial support of KAU.

pollution control), and in defense and military technology (e.g., surveillance against new types of biological and chemical attacks at the nanoscale).

The peculiarities of nanosensors introduce many challenges in the realization of WNSNs. On the one hand, the miniaturization of classical antennas to meet the size requirements of nanosensors would impose the use of very high operating frequencies (hundreds of Terahertz), which would limit the feasibility of WNSNs. To overcome this limitation, the use of graphene-based nano-antennas and nano-transceivers has been recently proposed [10,23,17,25]. As a result, nanosensors are expected to communicate in the Terahertz Band (0.1–10 THz). The Terahertz Band suffers from a very high propagation loss, which drastically limits the communication range of nanosensors due to their expectedly very limited power and energy. At the same time, though, it provides a very large bandwidth, which can be used to develop simple but yet efficient modulation and medium sharing schemes.

On the other hand, the very limited amount of energy that nano-batteries can hold and the unfeasibility to manually recharge or replace them, have motivated the development of novel nanoscale energy harvesting systems [27,6,4]. Nanoscale power generators convert vibrational, fluidic, electromagnetic or acoustic energy into electrical energy. When using energy harvesting systems, the energy of nanosensors does not just decrease with time, but has both positive and negative fluctuations. Therefore, rather than minimizing the energy consumption, a communication system should optimize the use of the energy in the nano-battery by capturing its temporal fluctuations. Ultimately, WNSNs can achieve perpetual operation if the energy consumption process and the energy harvesting process are jointly optimized.

Due to the transmission at very high speed in the Terahertz Band and the expectedly very high number of nanosensors in WNSNs willing to simultaneously communicate, novel Medium Access Control (MAC) protocols are needed to regulate the access to the channel and to coordinate and synchronize the transmissions among nano-devices. Classical MAC protocols cannot directly be used in WNSNs because they do not capture (i) the limited processing capabilities of nanosensors, which requires the development of ultra-low-complexity protocols [2]; (ii) the peculiarities of the Terahertz Band [12], i.e., very large distant-dependent bandwidth (bandwidth is not a problem anymore, but synchronization is) and very high propagation loss (very limited transmission range); and, (iii) temporal energy fluctuations of nanosensors due to the behavior of power nano-generators [9]. Therefore, there is a need to revise the traditional assumptions in MAC design and propose new solutions tailored to this paradigm.

In this paper, we propose an energy and spectrum aware MAC protocol to achieve perpetual WNSNs. First, we propose to take advantage of the hierarchical network architecture of WNSNs and shift the complexity of the MAC protocol towards more resourceful nano-controllers. In our solution, the nano-controller regulates the access to the channel of the nanosensors, by following a Time Division Multiple Access (TDMA) approach. To guarantee

a fair, throughput and lifetime optimal access to the channel, the nano-controller takes into account the data requirements and energy constraints of the different nanosensors willing to communicate. Moreover, this is done for two different possible physical layers, namely, a more practical physical layer based on a recent proposed pulse-based scheme for nanoscale communications, and a theoretical bandwidth-adaptive capacity-optimal physical layer. The system model and an overview of the proposed solution are explained in Section 3 and Section 4, respectively.

As the essential building block of the proposed MAC solution, the throughput-and-lifetime optimal schedule has to be designed, which aims to find an optimal transmission order for the nanosensors so that the network throughput is maximized, while maintaining the infinite network lifetime. Towards this end, we first derive an important system design parameter, namely, the critical packet transmission ratio (CTR). The CTR is the maximum allowable ratio between the transmission time and the energy harvesting time, below which the nanosensor node can harvest more energy than the consumed one, thus achieving perpetual data transmission. Thanks to the peculiarities of the Terahertz Band and the nanoscale energy harvesting process, it is revealed that the CTR exhibits a unique distance-dependent nature so that nanosensors at different locations possess different CTR. The definition and the details on the computation of the CTR are explained in Section 5.

Based on the CTR, a novel symbol-compression based MAC solution, built on the pulse-based physical layer, is introduced. The symbol-compression solution utilizes the unique elasticity of the inter-symbol spacing to allow multiple nanosensors to transmit their packets in parallel without inducing any transmission collisions. Based on this symbol-compression solution, a sub-optimal symbol-compression scheduling algorithm is proposed, which can assign each nanosensor with different sets of transmission slots in such a way that all nanosensors achieve their near-maximum single-user throughput, simultaneously, while maintaining their transmission ratios below the CTR for energy balancing. Different from the pulse-based physical layer, we reveal that there exist three unique properties of the capacity-optimal physical layer, namely, (i) non-overlapped packet transmissions, (ii) nonexistence of throughput-and-lifetime optimal schedules, and (iii) the single-user throughput unbalance. Then, based on these properties, a packet-level timeline scheduling algorithm is proposed to achieve the balanced single-user throughput with the infinite network lifetime. The algorithms are presented in Section 6.

The remainder of this paper is organized as follows. In Section 2, we review the recent literature related to MAC protocols for WNSNs. In Section 3, we describe the nanosensor model and network model used in our analysis. In Section 4, we provide an overview of the proposed energy and spectrum-aware MAC protocol. In Section 5, we analytically obtain the energy harvesting rate and the energy consumption rate for the two proposed physical layers, and compute the CTR. We present the optimal throughput

and lifetime scheduling algorithms in Section 6 and evaluate their performance in Section 7. Finally, we conclude the paper in Section 8.

2. Related work

There are not many MAC solutions for WSNs for the time being. In [13], we proposed the PHLAME, the first MAC protocol for ad hoc nanonetworks. In this protocol, nano-devices such as nanosensors are able to dynamically choose different physical layer parameters based on the channel conditions and the energy of the nano-devices. These parameters were agreed between the transmitter nano-device and the receiver nano-device by means of a handshaking process. However, there are two limitations in the PHLAME. On the one hand, as shown in the paper, the use of a handshake process can limit the real potential of the Terahertz Band. On the other hand, nanosensors might not have enough computational resources to dynamically find the optimal communication parameters.

Existing MAC protocols for macroscale wireless sensor networks or ad hoc networks are not adequate for WSNs, because they do not capture the peculiarities of the Terahertz Band or the capabilities of nano-devices and, in particular, of nanoscale energy harvesting systems. On the one hand, for the time being and to the best of our knowledge, there are no MAC protocols for Terahertz Band communications. The closest wireless communication technology is the use of the 5 GHz transmission window at 60 GHz, which has been recently included in the IEEE 802.11ad [8,7]. This system adopts a very similar link layer as the entire IEEE 802.11 standard. However, it is well known that the use of the classical handshake process limits the achievable throughput and latency of this technology. The main reason for this is the fact that when transmitting at very high bit-rate and usually with directional antennas, interference problems (e.g., hidden terminal problem) are not the main constraint, but the main challenge is to achieve tight synchronization among the devices. Some other MAC protocols for 60 GHz communication systems can be found in the literature [24], but these are usually only minor deviations from the standard.

On the other hand, energy harvesting systems also affect the way in which MAC protocols should be designed. However, existing MAC protocols for energy harvesting Wireless Sensor Networks (WSNs) [22,28] do not capture the peculiarities of nanoscale energy harvesting systems. For example, in [22], the authors investigate the performance of SMAC in a solar-energy-powered WSN. In particular, the impact of the sensors duty cycle on the average energy in the sensors battery and the achievable throughput is investigated by starting from an analytical model of energy harvester. However, solar energy might not be always available to nanosensors, the efficiency of nanoscale photovoltaic cells remains unknown, and the physical layer of nanosensors is totally different to that of classical sensors. In [28], two dynamic duty-cycle scheduling schemes (called DSR and DSP) are described. In DSR, each

sensor node is permitted to fine-tune its duty-cycle based on the current amount of remaining energy only. Once again, however, this solution does not take the particular energy harvesting process at the nanoscale or the behavior of the Terahertz Band channel. From this, it is clear that a new MAC policy for WSNs is needed.

3. System model

In this section, we summarize the main peculiarities of nanosensors that affect the design of protocols for WSNs as well as the envisioned network model of WSNs.

3.1. Nanosensor model

The capabilities of nanosensors introduce major constraints in the design of protocols for WSNs. In particular,

- **Nanosensors will have very limited computational capabilities.** As a result, nanosensors are not capable of handling complicated communication protocols. Nanoprocessors are being enabled by the development of smaller transistors. The smallest transistor that has been experimentally tested to date is based on a thin graphene strip, which is made of just 10 by 1 carbon atoms [19]. These transistors are not only smaller, but also able to operate at much higher frequencies (up to a few THz). However, the complexity of the operations that a nanoprocessor will be able to handle depends on the number of transistors in the chip, thus, on its total size. We capture this peculiarity in our model by defining a hierarchical network architecture and shifting the protocol complexity from the nanosensors to more resourceful nano-controllers [2], as we will explain in Section 3.2.
- **Nanosensors will be able to communicate over the Terahertz Band (0.1–10 THz)** by using novel nano-antennas [10,15,23] and nano-transceivers [5,17,21,25], which exploit the unique properties of novel nanomaterials such as graphene. The Terahertz Band channel supports the transmission at very high bit-rates (up to a few Terabits per second) but only over very short distances (below 1 m) [12,18]. Due to molecular absorption, i.e., the process by which part of the EM energy of a wave is converted into kinetic energy internal to vibrating gaseous molecules, the available transmission bandwidth of the Terahertz Band shows a very unique distance-dependent behavior. In particular, the available transmission bandwidth can shrink from almost 10 THz at few millimeters to just a few tens of Gigahertz at a few centimeters. We capture this peculiarity in our model by considering novel bandwidth-adaptive communication schemes, as we will explain in Section 5.
- **Nanosensors will require energy harvesting nano-systems for continuous operation.** The amount of energy that can be stored in the nanosensor batteries is extremely low. As a result, nanosensors can only complete a very few tasks with a single battery charge. Due to the impossibility to manually recharge or replace the batteries of the nanosensors, novel energy harvesting nano-systems have been developed [27,6,4]. In contrast to the classical battery-powered

devices, the energy of the self-powered devices does not just decrease until the battery is empty, but it has both positive and negative fluctuations. As a result, the lifetime of energy harvesting networks can tend to infinity provided that the energy harvesting and the energy consumption processes are jointly designed. We capture this peculiarity in our model by jointly analyzing the energy consumption process due to communication in the Terahertz Band and the energy harvesting process by means of a piezoelectric nano-generator, as we explain in Section 5.

3.2. Network model

Due to the limitations of individual nanosensors, in order to enable large-scale nanosensor networks, a hierarchical network architecture is required, where the whole network is partitioned into a set of clusters. Each cluster is locally coordinated by a nanocontroller with more advanced capabilities and, thus, the complexity of any protocol or algorithm can be pushed towards the nanocontroller side. In addition, the nano-controller can be used to guarantee the required physical layer synchronization for communication at very high data-rates in the Terahertz Band. As first described in [2], the nano-controller is expected to have more capabilities than a simple nanosensor, at the expense of a much larger size.

4. Overview of energy and spectrum-aware MAC

The Terahertz Band supports the transmission at very high bit-rates. MAC protocols that involve heavy signaling (e.g., classical handshaking process with conventional *RequestToSend* and *ClearToSend* packet exchange) may limit the achievable throughput of Terahertz Band communication networks, especially if an external device, in this case the nanocontroller, can take care of the synchronization among nano-devices. For this, we propose a dynamic scheduling scheme based on TDMA, which is tailored to the capabilities of the nanosensors and the peculiarities of the Terahertz Band.

In this scheme, each nanosensor is dynamically assigned variable-length transmission time slots. The length of the slots is related to the amount of data it needs to transmit, the distance and channel conditions between the nanosensor and the nanocontroller, and the energy in the battery of the nanosensor, as we will detail next. When not transmitting, the nanosensor is sleeping. The energy harvesting process by which the nanosensors can replenish their batteries is performed in both transmission and sleeping timeslots. The objective is to optimally assign transmission and sleeping timeslots among nanosensors in such a way that the harvested energy and the consumed energy are balanced for each nanosensor, thus leading to infinite network lifetime. Besides the everlasting network operation, the proposed scheduling algorithm also needs to ensure the throughput optimality so that all nanosensors can achieve their respective maximum single-user throughput simultaneously.

Before determining how the time slots can be optimally allocated to different nanosensors, we define the time frame structure considered in our analysis. Each frame is divided in three fixed-length sub-frames: *Down Link* (DL), *Up Link* (UL) and *Random Access* (RA). In the DL, the nanocontroller broadcasts (BC) general information and can also send targeted data or commands to specific nanosensors. Different nanosensors have slots with different lengths. The DL can also be used to send wake up preambles to activate specific nanosensors or all of them (BC). In the UL, nanosensors send data to the nanocontroller. As in the DL, different nanosensors might have slots with different lengths. Finally, in the RA, nanosensors can require the slots to the nanocontroller for the next frame, or can exchange information among them in an ad hoc fashion if the protocol supports it.

In our analysis, we focus on the UL, as the transmission of information is the process that is most affected by the power and energy limitations of nanosensors. In our scenario, when nanosensor that needs to transmit data to the nanocontroller will inform the latter by sending a request in the RA sub-frame. The transmission request should specify the nanosensor ID, amount of data, and remaining energy. On its turn, the nanocontroller will use the received request as well as the measured channel conditions to optimally determine the way that the nanosensor should proceed. This is notified to the nanosensor in the next frame DL.

5. Critical packet transmission ratio

Since all the nanosensors should directly communicate with the nanocontroller, to achieve the above design objectives (not to consume more energy than the available one and make sure a fair use of the resources among nanosensors), we need first to derive the critical packet transmission ratio (CTR) at different distances. The CTR is defined as the ratio between the duration of the transmission slot and the total duration of the transmission timeslot and the sleeping timeslot. Below this CTR, the sensor node can harvest more energy than the consumed one, thus achieving perpetual data transmission.

To determine the CTR, we need to evaluate the packet energy consumption rate and packet energy harvesting rate, respectively. In our analysis, we consider two different communication schemes to compute the energy consumption rate. First, we consider TS-OOK [11], a recently proposed communication scheme for nano-devices based on the transmission of femtosecond-long pulses by following an on-off keying modulation spread in time. Second, we consider the use of a capacity-optimal communication scheme, which will serve to determine the upper bound in terms of performance.

5.1. Energy consumption rate for TS-OOK-based communication

In light of the state of the art in graphene-based nanoelectronics, we consider first the use of TS-OOK [11], a recently proposed communication scheme for nano-devices,

which is based on the transmission of very short pulses, just one-hundred-femtosecond long, by following an on-off keying modulation spread in time. These pulses can be generated and detected with compact nano-transceivers based on graphene and high-electron-mobility materials such as Gallium Nitride or compounds of Gallium-Arsenide [14,20,17,1,26].

The functioning of TS-OOK is as follows. The symbol “1” is transmitted by using a one-hundred-femtosecond-long pulse and the symbol “0” is transmitted as silence, i.e., the nano-device remains silent. The time between symbols t^s is much longer than the symbol duration t^p , i.e., $\beta = t^s/t^p \gg 1$. The reason for this is twofold. On the one hand, due to technology limitations, pulses cannot be emitted in a burst. On the other hand, the separation of pulses in time allows for the relaxation of the vibrating molecules in the channel [12]. During the time between symbols, a device can either remain idle or receive other incoming information flows. Therefore, TS-OOK enables simple multiple-access policies.

We next derive the energy consumption rate when using TS-OOK. First, the energy per pulse in TS-OOK is constant and equal to E^p . This value is a technology constraint and, according to the state of the art in Terahertz Band pulse emitters [14,20,17,1,26], E^p is in the order of a few aJ (10^{-18} J). This value corresponds to a peak pulse transmission power in the order of a few μ W. Note that, during the transmission of “0”s, no energy is consumed.

From [11], the maximum achievable information rate \mathcal{IR} with TS-OOK in bit/symbol as a function of the transmission distance d is given by,

$$\begin{aligned} \mathcal{IR}(d) = \max_X \left\{ - \sum_{m=0}^1 p_m \log_2 p_m \right. \\ \left. - \int \sum_{m=0}^1 \frac{p_m}{\sqrt{2\pi}N_m} \exp\left(-\frac{1}{2} \frac{(y - a_m(d))^2}{N_m(d)}\right) \right. \\ \cdot \log_2 \left(\sum_{n=0}^1 \frac{p_n}{p_m} \sqrt{\frac{N_m(d)}{N_n(d)}} \right) \\ \left. \cdot \exp\left(-\frac{1}{2} \frac{(y - a_n(d))^2}{N_m(d)} + \frac{1}{2} \frac{(y - a_m(d))^2}{N_m(d)}\right) dy \right\}, \quad (1) \end{aligned}$$

where $X = \{p_0, p_1\}$ refers to the transmitter source probability distribution, p_m refers to the probability of transmitting symbol $m = \{0, 1\}$, i.e., the probability to stay silent or to transmit a pulse, respectively, and a_m and N_m stand for the amplitude of the received symbol and the total noise power associated to the transmitted symbol m , which depend on the transmission distance and are obtained by using the Terahertz Band channel model in [12]. Note that \mathcal{IR} is not always achieved for the equiprobable source distribution ($p_0 = p_1 = 0.5$). This is a consequence of the Terahertz Band channel asymmetric noise behavior [11].

Based on these, we define the energy consumption rate $\lambda_{con-tsook}$ in J/s as

$$\lambda_{con-tsook}(d) = \lambda_{bit}(d) \frac{1}{\mathcal{IR}(d)} E_{pulse} \hat{p}_1(d), \quad (2)$$

where λ_{bit} is the transmission bit-rate in bit/s, \mathcal{IR} is the achievable information rate in bit/symbol, E_{pulse} is the energy per pulse consumption and \hat{p}_1 is the optimal probability to transmit a pulse for which the \mathcal{IR} is achieved. Note that λ_{bit} should not exceed the achievable information rate in bit/s, i.e.,

$$\lambda_{bit}(d) \leq R_{tsook}(d) = \frac{B}{\beta} \mathcal{IR}(d), \quad (3)$$

where B is the maximum bandwidth (i.e., 10 THz in our analysis), β is the spreading factor, and R_{tsook} is the maximum transmission rate in bit/s and \mathcal{IR} is the maximum achievable information rate in bit/symbol given by (1).

5.2. Energy consumption rate for capacity-optimal bandwidth-adaptive communication

Aimed at obtaining theoretical bounds for the performance of our MAC solution for WSNs, we consider next the use of a capacity-optimal bandwidth-adaptive communication scheme. Indeed, the Terahertz Band channel has a very peculiar behavior with distance. On the one hand, as in any wireless communication scheme, the path-loss suffered by a propagating signal increases with the transmission distance. Therefore, as the distance between a nanosensor and the nanocontroller increases, a higher power is needed to guarantee a target Signal-to-Noise Ratio (SNR) at the receiver. On the other hand, due to molecular absorption, the available transmission bandwidth drastically decreases with distance. As a result, a longer transmission time is needed to transmit the same amount of information. Therefore, the energy per bit consumption increase with distance is twofold, i.e., a higher power is needed over a longer timeslot.

In order to mathematically capture this behavior, we proceed as follows. In this first case, we consider that nanosensors can make use of dynamic power control. Therefore, the transmission power P to guarantee a target SNR at the receiver is given by

$$P(d) = \int_{B_{3dB}(d)} S(d, f) df = SNR \int_{B_{3dB}(d)} A(d, f) S_N(d, f) df, \quad (4)$$

where d refers to the transmission distance, B_{3dB} is the 3 dB bandwidth, S_{opt} is the optimal power spectral density (p.s.d.) of the transmitted signal, f stands for frequency, A is total path-loss and S_N is the noise p.s.d.

The total path-loss A in (4) can be written as [12]

$$A(d, f) = \left(\frac{c}{4\pi d f_0} \right)^2 \exp(-k(f)d), \quad (5)$$

where d refers to the transmission distance, f stands for the frequency, f_0 is the design center frequency, c is the speed of light in the vacuum, and k is the molecular absorption coefficient,

$$k(f) = \sum_i \frac{p}{p_0} \frac{T_{STP}}{T} Q^i \sigma^i(f), \quad (6)$$

where p refers to the system pressure in Kelvin, p_0 is the reference pressure, T_{STP} is the temperature at standard pressure, Q^i is the number of molecules per volume unit

of gas i and σ^i is the absorption cross-section of gas i . More details on how to compute the molecular absorption cross-section σ can be found in [12].

The noise in the Terahertz Band is mainly contributed by the molecular absorption noise. This type of noise is generated by vibrating gaseous molecules which reradiate part of the energy that have been previously absorbed. Therefore, this noise is correlated to the transmitted signal. From [12], the total molecular absorption noise p.s.d. S_N is contributed by the atmospheric noise S_{N_0} [3] and the induced noise S_{N_1} , and can be obtained as

$$S_N(d, f) = S_{N_0}(d, f) + S_{N_1}(d, f), \quad (7)$$

$$S_{N_0}(f) = \lim_{d \rightarrow \infty} k_B T_0 (1 - \exp(-k(f)d)) \left(\frac{c}{\sqrt{4\pi f_0}} \right)^2, \quad (8)$$

$$S_{N_1}(d, f) = S(f) (1 - \exp(-k(f)d)) \left(\frac{c}{4\pi d f_0} \right)^2, \quad (9)$$

where d refers to the transmission distance, f stands for the frequency, k_B is the Boltzmann constant, T_0 is the room temperature, k is the molecular absorption coefficient in (6), c is the speed of light in the vacuum, f_0 is the design center frequency, and S is the p.s.d. of the transmitted signal.

The 3 dB bandwidth B_{3dB} as a function of the transmission distance d is defined as the range of frequencies such that

$$\{f | A(d, f) S_N(d, f) \leq 2A(d, f_0(d)) S_N(d, f_0(d))\}, \quad (10)$$

where f_0 is the center frequency and also depends on the transmission distance.

To compute the capacity of the Terahertz Band under this scheme, we proceed as follows. First, note that the induced noise N_1 (9) depends on the p.s.d. of the transmitted signal S as well as on the absorption coefficient of the channel k . By properly selecting S , S_{N_1} can become negligible and thus $S_N \approx S_{N_0}$. Similarly to the water filling principle, by allocating the power of the transmitted signal only at those frequencies at which the resulting noise is lower, we can maximize the achievable information rate or capacity. By considering the resulting molecular absorption noise in (7) to be additive and Gaussian, the maximum transmission bit-rate C can be written as

$$\begin{aligned} C(d) &= \int_{B_{3dB}(d)} \log_2 \left(1 + \frac{S(d, f) A^{-1}(d, f)}{S_{N_0}(d, f)} \right) df \\ &= B_{3dB}(d) \log_2(1 + \text{SNR}), \end{aligned} \quad (11)$$

where B_{3dB} stands for the 3 dB bandwidth in (10), S is the power spectral density of the transmitted signal, A is the channel path-loss and S_{N_0} is the noise p.s.d.

The average energy per bit consumption $E_{bit-opt}$ as a function of the transmission distance d can be obtained as

$$E_{bit-opt}(d) = \frac{P(d)}{C(d)} = \frac{\text{SNR} \int_{B_{3dB}(d)} A(d, f) S_{N_0}(d, f) df}{B_{3dB}(d) \log_2(1 + \text{SNR})}. \quad (12)$$

Finally, we define the energy consumption rate $\lambda_{con-opt}$ in J/s for the optimal communication scheme as

$$\lambda_{con-opt}(d) = \lambda_{bit}(d) E_{bit-opt}(d), \quad (13)$$

where d refers to distance, λ_{bit} is the bit transmission rate and $E_{bit-opt}$ is the energy per bit consumption in (12). Note that λ_{bit} should not exceed the transmission rate R_{opt} or capacity of the system given by (11):

$$\lambda_{bit}(d) \leq R_{opt}(d) = C(d). \quad (14)$$

5.3. Energy harvesting rate

As introduced in Section 3, nanosensors require energy harvesting systems to replenish their batteries. Amongst others, one of the main alternatives is to use novel piezoelectric nano-generators [27]. A piezoelectric nano-generator converts vibrational and kinetic energy into electricity by exploiting the piezoelectric behavior of Zinc Oxide nanowires. Every time that the ZnO nanowires are compressed or released, a small electric current is generated. This can be used to recharge an ultra-nano-capacitor after proper rectification. Our starting point for our analysis is the model introduced in [9], which can accurately reproduce experimental measurements.

We are interested in the energy harvesting rate, i.e., the speed at which the battery is replenished, λ_{harv} . The energy in battery can be written as

$$E_{batt} = \frac{1}{2} V_g^2 C_{cap} \left(1 - \exp \left(- \frac{\Delta Q}{V_g C_{cap}} n_{cycle} \right) \right), \quad (15)$$

where V_g is the generator voltage, C_{cap} refers to the ultra-nano-capacitor capacitance, and ΔQ is the electric charge harvested per cycle.

From this, the energy harvesting rate in J/s is obtained as:

$$\begin{aligned} \lambda_{harv} &= \lambda_{cycle} \frac{\partial E_{batt}}{\partial n_{cycle}} \\ &= \frac{1}{2} C_{cap} V_g^2 \left(2 \frac{\Delta Q}{V_g C_{cap}} \exp \left(- \frac{\Delta Q}{V_g C_{cap}} n_{cycle} \right) \right. \\ &\quad \left. - 2 \frac{\Delta Q}{V_g C_{cap}} \exp \left(- 2 \frac{\Delta Q}{V_g C_{cap}} n_{cycle} \right) \right), \end{aligned} \quad (16)$$

where λ_{cycle} is the vibration frequency or compression-release rate of the ZnO nanowires, and the rest of parameters have already been defined.

5.4. Critical packet transmission ratio

The CTR λ^c can be obtained by taking into account that the energy harvested during a time slot of length T is larger than the energy consumed during the transmission time T_{tx} :

$$\lambda_{harv} T \geq \lambda_{con} T_{tx}. \quad (17)$$

Thus,

$$\lambda^c(d) = \frac{\lambda_{harv}}{\lambda_{con}(d)} \quad (18)$$

where $\lambda_{con} = \lambda_{con-opt}$ in (13) for capacity-optimal communication and $\lambda_{con} = \lambda_{con-tsook}$ in (2) for TS-OOK-based communication.

6. Throughput-and-lifetime optimal scheduling

As introduced in the previous section, the critical packet transmission ratio determines the percentage of time a nanosensor can transmit so that it can ensure the balance between the harvested and the consumed energies. In this section, based on this CTR, we study the throughput-and-lifetime optimal scheduling problem, which aims to find an optimal transmission schedule for the nanosensors so that the network throughput is maximized, while maintaining the infinite network lifetime. To this end, we propose the optimal scheduling algorithms for TS-OOK-based and capacity-optimal nano-communication, respectively. The proposed algorithms can assign each nanosensor with different sets of transmission slots in such a way that all nanosensors achieve their maximum single-user throughput, simultaneously, while maintaining their transmission ratios below the critical ones for energy balancing. Specifically, the throughput-and-lifetime optimal scheduling problem can be formally defined as follows. First, the following notations are introduced.

- S_i the transmission schedule of sensor i
- R_i the maximum achievable data rate of sensor i
- $s_{i,j}$ the start time of the j th packet of sensor i in S_i
- $f_{i,j}$ the finish time of the j th packet of sensor i in S_i
- Γ the total transmission schedule, i.e., $\Gamma = \bigcup_{i \leq M} S_i$
- L^Γ the length of the transmission schedule
- N_i^Γ the total number of packets sent by sensor i in Γ

Definition 1 (*Total Transmission Schedule*). Let the transmission schedule S_i of each nanosensor n_i be denoted by a triplet

$$S_i \left(s_{i,j}, f_{i,j \leq N_i^\Gamma}, N_i^\Gamma \right). \quad (19)$$

Then, the total transmission schedule can be defined as

$$\Gamma = \left\{ S_i \left(\{s_{i,j}, f_{i,j}\}_{j \leq N_i^\Gamma}, N_i^\Gamma \right) \right\}_{i \leq M}. \quad (20)$$

Definition 2 (*Maximum single-user throughput*). The maximum single-user throughput \mathcal{A} is defined as the maximum data rate a nanosensor can achieve to guarantee the infinite network lifetime, i.e., for a nanosensor i at a distance d_i from nanocontroller

$$\mathcal{A}_i = R_i \lambda^c(d_i), \quad (21)$$

where $\lambda^c(d_i)$ is the CTR given in (18) and R_i is the maximum achievable data rate, i.e., $R_i = R_{opt}$ for capacity optimal communication given in (14) and $R_i = R_{tsook}$ for TS-OOK communication given in (3).

Now, the throughput-and-lifetime optimal scheduling can be formally defined as follows.

Definition 3 (*Throughput-and-Lifetime Optimal Scheduling (TLOS) problem*). Given M nanosensors, find a transmission schedule S_i for each nanosensor n_i so that the total transmission schedule Γ satisfies the following conditions

1. **Non-Collision**: no nanosensor starts its transmission during the transmissions of any other nanosensors.
2. **Throughput Optimality**: each nanosensor has a transmission schedule $S_i \in \Gamma$, by which it can achieve the maximum single-user throughput \mathcal{A}_i defined in Definition 2, i.e.,

$$(\exists \Gamma)(\forall n_i, i \leq M) : \frac{\sum_{j \leq N_i^\Gamma} (f_{i,j} - s_{i,j})}{L_\Gamma} = \lambda^c(d_i).$$

and consequently

$$\mathcal{A}_i = R_i \lambda^c(d_i), \forall n_i, i \leq M. \quad (22)$$

3. **Lifetime Optimality**: each nanosensor can sufficiently recharge itself so that it has enough energy for the next packet transmission, i.e.,

$$s_{i,j} - s_{i,j-1} \geq T_i, \forall i \leq M, j \leq N_i^\Gamma, \quad (23)$$

where T_i is the minimum transmission period (MTP) per packet for the balanced energy consumption and harvesting, i.e.,

$$T_i = \frac{N_{bits}}{R_i \lambda^c(d_i)}. \quad (24)$$

Remark 1. In the above definition, conditions (1) and (2) guarantee that the network throughput is maximized by allowing all the nanosensors approach their respective single-user throughput simultaneously, without allowing any inter-user transmission collisions. The condition (3) ensures that the nanosensor network has the infinite network lifetime by letting each nanosensor achieve the balanced energy consumption and harvesting.

In the rest of this section, we present the optimal algorithms to solve the throughput-and-lifetime optimal scheduling problem under two scenarios: (1) TS-OOK communication and (2) capacity-optimal communication.

6.1. Symbol-compression scheduling for TS-OOK

As introduced in Section 5.1, TS-OOK is a communication scheme based on the transmission of a train of very short symbols (pulse as “1” and silence as “0”) with fixed length equal to one hundred femtoseconds. However, as introduced in Section 5.1, the inter-symbol spacing t^s of TS-OOK, i.e., the time separation between two consecutive symbols, shows great elasticity. The unique elasticity of TS-OOK paves the way to a novel MAC scheme for nanosensor networks, namely, symbol-compression communication.

The basic idea of this scheme is that based on the inter-symbol spacing diversity of nanosensors, the packet transmissions of multiple nanosensors can be performed simultaneously or in parallel by compressing or interleaving the symbol transmissions of multiple nanosensors within a proper time interval. This interval is much shorter than the total time of sequentially sending each nanosensor's packet back to back. An example of symbol-compression communication is shown in Fig. 1. Consider two nanosensors with different transmission rates. By properly arranging the symbol transmission time, the two nanosensors can

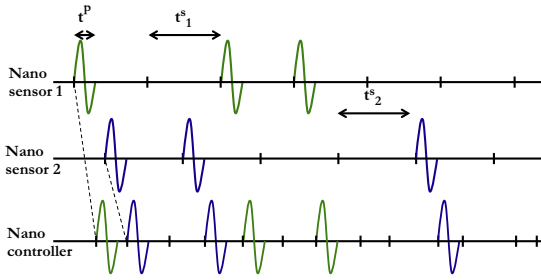


Fig. 1. Symbol-compression communication using TS-OOK.

transmit with their respective transmission rate without causing any symbol collisions.

Based on the symbol compression communication, we next propose a throughput and lifetime optimal scheduling algorithm by allocating the symbol transmissions of nanosensors in the optimal time instances so that the conditions given in Definition 3 are satisfied. The pseudo code of the proposed algorithm is given in Algorithm 1 with the steps summarized as follows.

Step I (Line 1–2 of Algorithm 1): for each nanosensor n_i , which is d_i away from nanocontroller, calculate the number of symbols (NoS) per packet N_i^s and the MTP per packet T_i . Specifically, we have

$$N_i^s = \frac{N_{bits}}{\mathcal{I}\mathcal{R}_i(d_i)}, \quad (25)$$

where $\mathcal{I}\mathcal{R}_i(d_i)$, given in (1), is the maximum achievable information rate of nanosensor n_i with TS-OOK in bit/symbol. Combining (24) and (3) yields

$$T_i = \frac{N_{bits}\beta}{\mathcal{I}\mathcal{R}_i(d_i)B\lambda_i^c}, \quad (26)$$

where B is the maximum bandwidth, β is the spreading factor or ratio between the time between symbols t^s and the symbol duration t^p . Then, the rounded MTP T_i^* is defined as the nearest multiple of t^p , i.e.,

$$T_i^* = \left\lceil \frac{T_i}{t^p} \right\rceil t^p, \quad (27)$$

Consequently, the length of the transmission schedule L^T is defined as the least common multiple (LCM) of the rounded MTP of the nanosensors, i.e.,

$$L^T = LCM(T_1^*, T_2^*, \dots, T_M^*). \quad (28)$$

Step II (Line 3–5 of Algorithm 1): for each nanosensor n_i , define the transmission period per symbol (TPPS) as follows

$$T_i' = \frac{T_i^*}{N_i^s - 1}, \quad (29)$$

which, by combining (25) and (27), yields

$$T_i' = \left\lceil \frac{N_{bits}t^s}{B\mathcal{I}\mathcal{R}_i(d_i)\lambda_i^c t^p} \right\rceil \frac{t^p \mathcal{I}\mathcal{R}_i(d_i)}{N_{bits}}, \quad (30)$$

where B is the maximum bandwidth (i.e., 10 THz in our analysis). Arrange nanosensors $\{n_1, \dots, n_M\}$ in a decreasing order of T_i , i.e., if $i < j$, then $T_i > T_j$. Then, assign each nanosensor n_i a priority $p_i = i$. By this way, the sensor with the longest TTPS T_i' has the lowest priority p_i .

Step III (Line 6–16 of Algorithm 1): assume the symbol of each nanosensor n_i arrives at the period T_i' . For each time slot τ_j of the schedule Γ , the nanocontroller decides which sensor has the right to transmit during τ_j , based on its associated counter $count_i$ and priority p_i . Specifically, among all nanosensors with nonzero $count_i$, the nanosensor with the highest priority p_i owns the transmission right during τ_j and thus τ_j is assigned to the transmission schedule S_i of nanosensor n_i . Initially, all counters $\{count_i\}$ are set as zero and then $count_i$ is updated at every time slot τ_j . If a symbol of nanosensor n_i arrives during τ_j , set $C_i = 1$. Otherwise, two scenarios can happen. If nanosensor n_i wins the transmission right during τ_j , then set $count_i = 0$, and otherwise, keeps $count_i$ unchanged.

Algorithm 1. Symbol-Compression Scheduling

-
- 1: Compute N_i^s and $T_i, \forall n_i \in M$;
 - 2: $T_i^* \leftarrow \left\lceil \frac{T_i}{t^p} \right\rceil t^p; L^T \leftarrow LCM(T_1^*, \dots, T_M^*)$
 - 3: $T_i' \leftarrow \frac{T_i^*}{N_i^s}$
 - 4: $\{\{n_i\}_{i \in M} | T_i' < T_j', \forall i > j\}$
 - 5: $p_i \leftarrow i, \forall i \in M$
 - 6: Associate each sensor n_i with a schedule S_i and a counter $count_i$
 - 7: $j \leftarrow 0; S_i \leftarrow \emptyset, count_i \leftarrow 1, \forall i \in M$
 - 8: **while** $jt^p \leq L^T$ **do**
 - 9: **if** $p_i == \max_{i \in M} p_i$ and $count_i == 1$ **then**
 - 10: $S_i \leftarrow S_i \cup \{\tau_j\}; count_i \leftarrow 0$
 - 11: **end if**
 - 12: **if** $\exists m \in M^+ : jT^s \leq mT_i' \leq (j+1)T^s$ **then**
 - 13: $count_i \leftarrow 1$
 - 14: **end if**
 - 15: $j \leftarrow j + 1$
 - 16: **end while**
-

The following Theorem defines the conditions under which the proposed symbol-compression algorithm lead to a **throughput and lifetime near optimal schedule**, i.e., each nanosensor has unlimited lifetime with the near-optimal transmission ratio λ_i^* , i.e.,

$$\lambda_i^* = \frac{N_i^s - 1}{N_i^s} \lambda_i^c(d_i) \quad (31)$$

and the near-maximum single-user throughput A_i^* , i.e.,

$$A_i^* = \lambda_i^* R_i = \frac{N_i^s - 1}{N_i^s} A_i, \quad (32)$$

where A_i is the maximum single-user throughput given in (21).

Theorem 1. Consider M nanosensors. The schedule Γ yielded from Algorithm 1 is throughput-and-lifetime near-optimal, if

$$\max_{i \leq M} \frac{t^p}{T_i^r} \leq \frac{1}{r+M} \text{ with } r = \frac{\max_{i \leq M} T_i^r}{\min_{i \leq M} T_i^r} \quad (33)$$

and T_i^r is the TPPS defined in (30).

Remark 2. The above Theorem implies that if the number of nanosensors is less than $1/(\max_{i \leq M} t^p / T_i^r) - r$, the symbol-compression algorithm can generate a throughput-and-lifetime near-optimal schedule. As shown in Fig. 2, T_i^r is of 10^4 order in picosecond and r , the ratio between the $\max(T_i^r)$ and $\min(T_i^r)$ is less than two. In addition, the symbol duration or the pulse width t^p can be as small as 0.1 picosecond. This means that the proposed scheduling algorithm can allow a large number of nanosensors (e.g., in the order of 10^5) to operate at their respective near-maximum single-user throughput.

Proof Theorem 1. First, it is easy to show that finding the throughput-and-lifetime near-optimal schedule is equivalent to finding the throughput and lifetime optimal schedule with the optimal throughput equal to A_i^* in (32). Then, we can show that the throughput-and-lifetime optimal scheduling (TLOS) problem (given in Definition 3) can be reduced into a non-preemptive periodic task scheduling (NPTS) problem. Next, we prove that the rate monotonic scheduling algorithm for NPTS is a generalized version of the proposed symbol-compression scheduling algorithm for TLOS. Consequently, the schedulability condition of the rate monotonic scheduling can lead to the optimality condition of the symbol-compression scheduling.

Given a set of nanosensors $\{n_i\}_{i \leq M}$, for each nanosensor n_i , we first convert the throughput optimality and lifetime optimality defined in Definition 3 into a periodic task model $tk_i(T_i^A, T_i^E, T_i^D)$, where T_i^A is the task arrival period, T_i^E is the task execution time and T_i^D is the relative deadline of the task, which is the maximum allowable time between the task arrival and the task completion. Because our

algorithm is a symbol-level scheduling approach, each task represents a symbol. Then, the symbol transmissions of all the nanosensors can be denoted by a set of periodic tasks, i.e.,

$$TK = \{tk_i(T_i^A, T_i^E, T_i^D), i = 1, 2, \dots, M\}. \quad (34)$$

Consider a particular nanosensor n_i , it has N_i^s symbols per packet. First, we have

$$T_i^E = t^p. \quad (35)$$

Then, according to Definition of 3(2), to guarantee the throughput optimality, it is sufficient to let nanosensor n_i finish sending N_i^s symbols for every T_i seconds, where T_i is the minimum transmission period (MTP) given in (24). This implies

$$T_i^A = \frac{T_i}{N_i^s} \text{ and } T_i^D = T_i^A \quad (36)$$

and if the deadline T_i^D can be met for every task, by combining (36) and (24), it follows that nanosensor n_i can achieve the maximum single-user throughput, i.e.,

$$A_i^* = \frac{T_i^E}{T_i^D} R_{\text{tsook}}(d_i) = \frac{N_i^s t^p}{T_i} = A_i. \quad (37)$$

Next, according to Definition of 3(3), to guarantee the lifetime optimality, it is sufficient to ensure the following two conditions are met: (1) the time difference T_i^s between the first symbol of n_i 's current packet and that of its previous packet is larger than T_i ; (2) the symbol transmissions of n_i are evenly scattered within T_i^s . To this end, we let

$$T_i^D = \frac{T_i}{N_i^s - 1}, \quad (38)$$

which ensures that under any scheduling algorithms, it follows

$$T_i^s = N_i \frac{T_i}{N_i^s - 1} > T_i. \quad (39)$$

For the sake of design simplicity, let

$$T_i^A = T_i^D = \frac{T_i}{N_i^s - 1}, \quad (40)$$

This, combining (29) and the fact that

$$T_i \gg t^p \text{ and } T_i^* = \left\lceil \frac{T_i}{t^p} \right\rceil t^p \approx T_i, \quad (41)$$

yields

$$T_i^D \approx T_i^*. \quad (42)$$

If every task is finished before the deadline T_i^D , it follows by combining (40) and (24) that n_i achieve near-maximum single-user throughput

$$A_i^* = \frac{T_i^E}{T_i^D} R_{\text{tsook}}(d_i) = \frac{(N_i^s - 1)t^p}{T_i} = \frac{N_i^s - 1}{N_i^s} A_i. \quad (43)$$

Finally, according to Definition of 3(1), to guarantee non-collisions among nanosensors, preemptions are not allowed during any scheduling algorithms, which means as

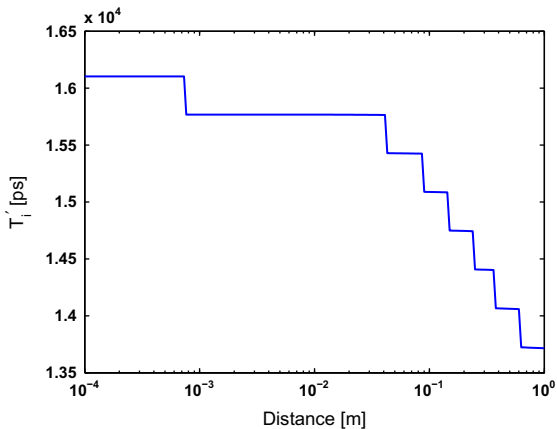


Fig. 2. The transmission period per symbol (TPPS) as a function of distance.

long as a nanosensor begins to transmit a symbol, during this symbol transmission, no other nanosensors can be scheduled to transmit.

Based on the above modeling, finding a throughput-and-lifetime near-optimal schedule is equivalent to solving the non-preemptive periodic task scheduling problem, which aims to find a *feasible* task schedule for the task set $TK = \{tk_i(T_i^A, T_i^E, T_i^D), i = 1, 2, \dots, M\}$, by which all tasks complete their execution before their respective deadlines, while no preemptions are allowed. Given a task set, it has been proven in [16] that the rate monotonic scheduling algorithm, which assigns the highest priority to the task with the shortest deadline T_i^D , is effective to find the feasible schedule. Based on the pseudo code in Algorithm 1, it can be shown that the proposed symbol-compression algorithm can be reduced to the rate monotonic scheduling algorithm. According to Theorem 4 in [16], a task set $TK = \{tk_i(T_i^A, T_i^E, T_i^D), i = 1, 2, \dots, M\}$ is schedulable under the rate monotonic scheduling, i.e., there is a feasible schedule for the task set by performing the rate monotonic scheduling, if

$$\max_{i \leq M} \frac{T_i^E}{T_i^D} \leq \frac{1}{r + M} \quad \text{with } r = \frac{\max_{i \leq M} T_i^D}{\min_{i \leq M} T_i^D}. \quad (44)$$

This, combining (35) and (42) completes the proof. \square

6.2. Timeline scheduling for capacity-optimal communication

In this section, we first present three properties of the capacity-optimal communications, namely, (1) non-overlapped packet transmissions, (2) nonexistence of throughput-and-lifetime optimal schedules, and (3) single-user throughput unbalance. Then, based on these properties, we propose a packet-level timeline scheduling algorithm to achieve the balanced single-user throughput with the infinite network lifetime.

6.2.1. Non-overlapped packet transmissions

Different from the pulse-based communication, the capacity-optimal communication cannot perform symbol-level scheduling because the waveform that conveys the symbols has to be arbitrary so that the maximum transmission bit-rate given in (11) can be achieved. This implies that under the capacity-optimal communication, the transmission durations of different nanosensors cannot be overlapped. In other words, when one nanosensor is transmitting a packet, all other nanosensors are not allowed to transmit. Consequently, different from the symbol-level scheduling for pulse-based physical layer technique, the scheduling has to be performed on the packet-to-packet level for the capacity-optimal case.

6.2.2. Nonexistence of the throughput-and-lifetime optimal schedule

The following Theorem defines the conditions under which the throughput-and-lifetime optimal schedule does not exist under the capacity-optimal communication.

Theorem 2. *If there exists at least one nanosensor residing within the distance D of the nanocontroller, where*

$$D = \arg \max_{d > 0} \lambda_{harv} > \lambda_{con-opt}(d), \quad (45)$$

then no scheduling algorithms can yield the throughput-and-lifetime optimal schedule under the capacity-optimal communication.

Remark 3. The above Theorem indicates that there may exist an algorithm to generate the throughput-and-lifetime optimal schedule only if all nanosensors are at least D far away from the nanocontroller. However, because the miniature nature of nanosensors, generally, the nanosensors are deployed randomly. Therefore, it is impossible to prevent the nanosensors being deployed within the range of D of the nanocontroller. Moreover, the numerical analysis given in Fig. 4(a) in Section 7 shows that such D indeed exists for the capacity-optimal communication. This indicates that the throughput-and-lifetime optimal schedule normally do not exist under the capacity-optimal communication.

Remark 4. It is worth to notice that the condition given in (45) is also applicable for the nonexistence of throughput-and-lifetime optimal schedule for TS-OOK. However, the numerical analysis given in Fig. 3(a) in Section VII shows $\lambda_{harv} < \lambda_{con-opt}(d)$ holds for any $d > 0$. This means that the distance threshold D does not exist for TS-OOK. Therefore, given an arbitrary set of nanosensors with any deployment topology, the throughput-and-lifetime optimal schedule may exist.

Proof Theorem 2. Similar to the proof of Theorem 1, we model the packet transmissions of nanosensors as a set of periodic tasks $TK = \{tk_i(T_i^A, T_i^E, T_i^D), i = 1, 2, \dots, M\}$. Specifically, both the task arrival time T_i^A and task deadline T_i^D are equal to $T_i = N_{bits}/R_i \lambda^c(d_i)$, the minimum transmission period (MTP) per packet defined in (24). The task execution time T_i^E is equal to the packet transmission time of nanosensor i , i.e., $T_i^E = N_{bits}/R_i$. Based on this model, the task set TK is schedulable only if $\sum_{i \leq M} T_i^E/T_i^D \leq 1$. Since $T_i^E/T_i^D = \lambda^c(d_i)$, this implies that no throughput-and-lifetime optimal schedule exists if $\sum_{i \leq M} \lambda^c(d_i) > 1$. This, combining the fact $\lambda^c(d_i) = \lambda_{harv}/\lambda_{con-opt}$, completes the proof. \square

6.2.3. Single-user throughput unbalance

Theorem 2 indicates that under the capacity-optimal communication, the nanosensors can be divided into two groups: near-region sensors and far-region sensors. The near-region sensors, which are within the distance D of the nanocontroller, always have their energy harvesting rate λ_{harv} larger than their energy consumption rate $\lambda_{con-opt}$. This indicates that the near-region sensors can operate at their maximum achievable data rate without spending extra sleep time recharging their batteries. According to Definition 2, this implies that the maximum

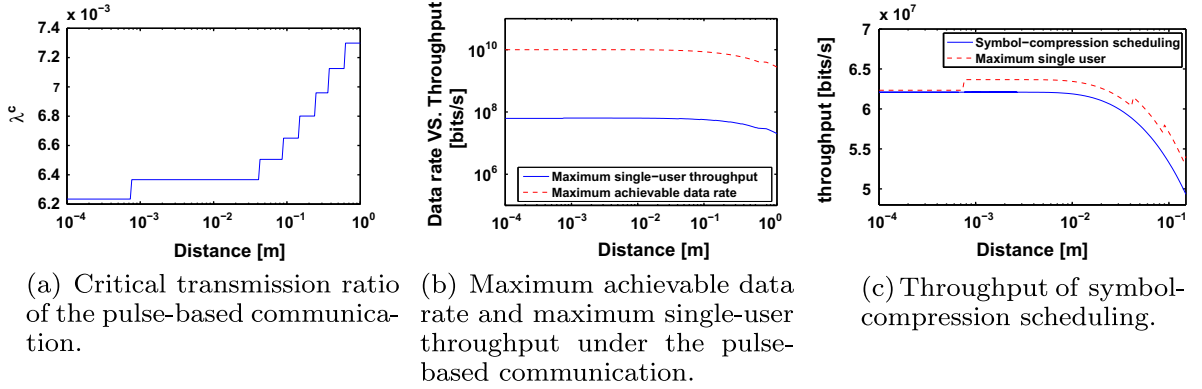


Fig. 3. Symbol compression scheduling for TS-OOK.

single-user throughput $A^{near}(d)$ of a near-region sensor can approach its maximum achievable data rate R_{opt} , i.e.,

$$A^{near}(d) = R_{opt}(d), \forall d < D. \quad (46)$$

In contrary to the near-region sensors, the far-region sensors, which are at least D far away from the nanocontroller, always have their energy harvesting rate λ_{harv} less than their energy consumption rate $\lambda_{con-opt}$. Therefore, the far-region sensors always need to enter the sleep state for recharging before their next packet transmissions. This implies that the far-region sensors have the maximum single-user throughput $A^{far}(d)$ necessarily smaller than the maximum achievable data rate R_{opt} , specifically,

$$A^{far}(d) = \lambda^c(d)R_{opt}(d), \forall d \geq D \quad (47)$$

Moreover, by analyzing R_{opt} given in (11), it is shown that the nanosensors at longer distance from the nanocontroller has the smaller maximum achievable data rate, i.e.,

$$R_{opt}(d_i) > R_{opt}(d_j), \forall d_i < d_j \quad (48)$$

In the light of (44)–(46), the maximum single-user throughput of the far-region nanosensors is much smaller than that of the near-region nanosensors, i.e.,

$$A^{near}(d_i) \gg A^{far}(d_i) \text{ with } d_i < D < d_j. \quad (49)$$

6.2.4. Packet-level timeline scheduling

Based on the properties of the capacity-optimal communication, we proposed a timeline scheduling algorithm, which decides the packet transmission order of the nanosensors at a set of discrete uneven time instants with an objective to ensure the infinite network lifetime with balanced single-user throughput between far-region sensors and near-region ones. The pseudo code of the proposed algorithm is given in Algorithm 2 with the steps summarized as follows.

Step I (Line 1–2 of Algorithm 2): calculate the minimum transmission period (MTP) per packet T_i for each nanosensors according to (24). Specifically, the near-region nanosensor has

$$T_i = N_{bits}/A^{near}(d_i) \quad (50)$$

and the far-region nanosensor has

$$T_i = N_{bits}/A^{far}(d_i). \quad (51)$$

Next, set the initial schedule length $L^I = \max_{i \leq M} T_i$. Let $d_{max} = \max_{i \leq M} d_i$. We have

$$L^I = N_{bits}/A^{far}(d_{max}). \quad (52)$$

Step 2 (Line 3–6 of Algorithm 2): associated each nanosensor n_i with a schedule S_i as defined in Definition 1. Set the packet counter in S_i as $N_i^I = 0$. Then, calculate the packet transmission time

$$T_i^{pk} = N_{bits}/R_{opt}(d_i) \quad (53)$$

for each nanosensor n_i . Next, arrange the nanosensors $\{n_i\}_{i \leq M}$ in the increasing order of the maximum single-user throughput A . Assign each nanosensor with a priority $p_i = i$, i.e., the nanosensor with smaller A has higher priority.

Step 3 (Line 7–14 of Algorithm 2): arrange the transmission order of nanosensors according to the priority p_i , the minimum transmission period (MTP) per packet T_i , and the packet counter N_i^I . At each schedule decision time τ , among all nanosensors with the smallest counter value, the nanosensor n_i is scheduled to transmit at τ if it satisfies three conditions. (1) It has the highest priority. (2) The backward difference between the current time τ and the start time of n_i 's previous packet is not smaller than its minimum transmission period (MTP) per packet T_i , i.e.,

$$\tau - s_{i,N_i^I} \geq T_i. \quad (54)$$

(3) The forward difference between the current time τ and n_i 's first packet transmission time is not smaller than its minimum transmission period (MTP) per packet T_i .

$$L^I - \tau + s_{i,1} \geq T_i \quad (55)$$

If n_i is scheduled to transmit at time τ , the next schedule decision time follows $\tau = \tau + T_i^{pk}$

Step 4: the step 3 is repeated until two conditions are met. (1) All nanosensors have been scheduled to transmit at least once, i.e., $N_i^f \geq 1, \forall i \leq M$. (2) the current schedule decision time τ_n is not smaller than the schedule length L^f

Algorithm 2. Timeline scheduling

```

1:  $\mathcal{A}_i \leftarrow \mathcal{A}^{near}(d_i)$ , if  $d_i < D$ ;  $\mathcal{A}_i \leftarrow \mathcal{A}^{far}(d_i)$ , if  $d_i \geq D$ ;
2:  $T_i \leftarrow N_{bits}/\mathcal{A}_i, \forall n_{i \leq M}; L^f \leftarrow \max(T_1, \dots, T_M)$ 
3:  $T_i^{pk} \leftarrow N_{bits}/R_{opt}(d_i), \forall n_{i \leq M}$ 
4:  $\{n\}_{i \leq M} \leftarrow \mathcal{A}_i < \mathcal{A}_j, \forall i < j$ 
5:  $p_i \leftarrow i, \forall i \leq M$ 
6:  $\tau \leftarrow 0; S_i \leftarrow \emptyset, N_i^f \leftarrow 0, \forall i \leq M$ 
7: while  $\tau \leq L^f$  and  $\exists i \leq M : N_i^f < 1$  do
8:   if  $N_i^f == \min_{i \leq M} N_i^f$  and  $p_i == \max_{i \leq M} p_i$  then
9:     if  $\tau - s_{i, N_i^f} \leftarrow T_i$  and  $L^f - \tau + s_{i, 1} \leftarrow T_i$  then
10:       $S_i \leftarrow S_i \cup \{s_{i, N_i^f} = \tau, f_{i, N_i^f} = \tau + T_i^{pk}\}$ ;
11:       $N_i^f \leftarrow N_i^f + 1; \tau \leftarrow \tau + T_i^{pk}$ ;
12:     end if
13:   end if
14: end while

```

7. Performance evaluation

In this section, we evaluate the performance of the proposed scheduling algorithms under the pulse-based physical layer and the capacity optimal physical layer, respectively. Specifically, we first analyze the critical transmission ratio and the maximum single-user throughput of the above mentioned two communication schemes. Then, we study the actual single-user throughput under the proposed scheduling algorithms, which approaches the maximum one.

In our numerical analysis, we use the following parameter values. Pulses in TS-OOK are modeled as the first time derivative of a one-hundred-femtosecond long Gaussian pulse with a total energy of 1 aJ (which corresponds to a peak power of 1 μ W). The Terahertz Band channel is modeled as in [12], for a standard gaseous medium with 10% of water vapor molecules. The piezoelectric energy harvesting system has the following parameters. We consider a capacitor with $C_{cap} = 9$ nF charged at $V_g = 0.42$ V for the computation of the energy in the nano-battery (15). For the computation of the energy harvesting rate λ_{harv} in (16), an ambient vibration with an average time between vibrations $t_{cycle} = 1/50$ s is considered. The amount of charge ΔQ harvested per cycle is 6 pC. The battery is fully discharged at the beginning of a simulation.

7.1. Symbol-compression scheduling for TS-OOK

As shown in Fig. 3(a), the critical transmission ratio of the pulse-based physical layer is always much less than one. This means that under the pulse-based communication, all nanosensors have to enter the sleep state for recharging

after each packet transmission. Moreover, Fig. 3(a) indicates that the sleeping time of the nanosensor is orderly longer than the transmission time. On one hand, this feature allow a large number of nanosensors to share the spectrum effectively without inducing inter-user collisions. On the other hand, the long sleeping time can lead to the reduced single-user throughput. Consequently, as shown in Fig. 3(b), the maximum achievable data rate is at least two order of magnitude higher than the maximum single-user throughput. However, in this case, the nanosensor can still achieve the data rate around 70 Mbits/s continuously.

Based on the above maximum single-user throughput, the proposed symbol-compression algorithm, shown in Algorithm 1, aims to find the optimal schedule so that all nanosensors can obtain their maximum single-user throughput simultaneously. To investigate the performance of the symbol-compression scheduling algorithm, we randomly select 160 nanosensors located within the radius of 0.15 m of the nanocontroller. Fig. 3(c) shows the single-user throughput yielded by the symbol-compression based scheduling algorithm. First, it is shown that the maximum single-user throughput is distance-dependent, which means the nanosensors closer to the noncontroller have higher maximum single-user throughput. This is due to the fact that under the pulse-based physical layer technique, all nanosensors utilize the equitant transmission power for the design simplicity and consequently the nanosensors closer to the nanocontroller have higher SNR, therefore leading to the higher throughput. Second, as shown in Fig. 3(c), the proposed symbol-compression algorithm can lead to the single-user throughput very close to the maximum one, which means that with the simple scheduling algorithm, all nanosensors can continuously and simultaneously convey their sensing data to the nanocontroller with very high data rate up to 60 Mbits/s.

7.2. Timeline scheduling for capacity-optimal communication

Now, we investigate the performance of the timeline scheduling algorithm under the capacity-optimal physical layer technique. As shown in Fig. 4(a), the critical transmission ratio of the capacity-optimal scheme shows the phase-transition phenomenon. More specifically, It is shown that there exists a distance D of around 0.04 m, above which the critical transmission ratio is less than one and below which the critical transmission ratio is larger than one. This phenomenon indicates that all nanosensors residing within D meter of the nanocontroller, a.k.a. the near-region nanosensors, can harvest more energy per second than the energy consumed for data transmission. Theretofore, all near-region nanosensors can transmit their data at full speed without entering the sleeping state for recharging. On the contrary, all nanosensors residing more than D meter far away from the nanocontroller, a.k.a. far-region nanosensors, have a critical transmission ratio less than one, therefore having to enter the sleeping state for recharging.

The above phase transition phenomenon can lead to the unbalanced single-user throughput for the nanosensors. As shown in Fig. 4(b), for the near-region nanosensors, their single-user throughput is equal to the maximum achiev-

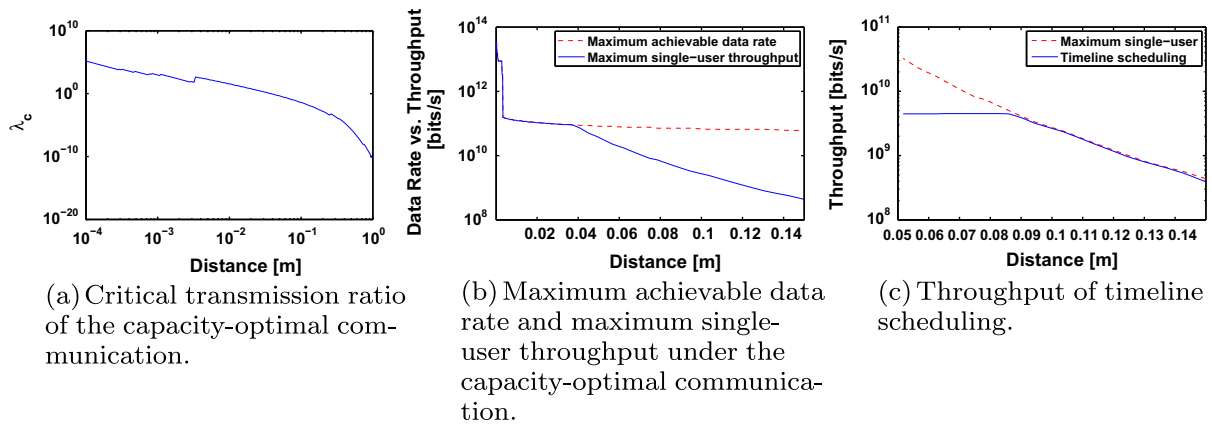


Fig. 4. Timeline scheduling for capacity-optimal communication.

able data rate. However, for the far-region nanosensors, their single-user throughput can be five order of magnitude smaller than their maximum achievable data rate. This means that the far-region nanosensors have orderly smaller throughput than the near-region ones. To encounter this problem, the proposed timeline scheduling aims to find the optimal schedule so that the far-region nanosensors can approach their maximum single-user throughput, while the near-region nanosensors can fairly share the spectrum in such way that they can achieve relatively equivalent throughput. As shown in Fig. 4(c), under the timeline scheduling, the nanosensors far away the nanocontroller can obtain the single-user throughput very close to the maximum achievable one, while the nanosensors close to the nanocontroller can achieve the same throughput. It is worth to notice that not all the near-region nanosensors can approach their maximum single-user throughput under the time-line scheduling algorithm. This is due to the fact that for any scheduling algorithm, given a set of nanosensors, the maximum single-user throughput is achievable for all nanosensors simultaneously only if the sum of the critical transmission ratios of the nanosensors is less than one. This condition is very difficult to satisfy when the number of near-region nanosensors increases.

8. Conclusions

WNSNs will boost the applications of nanotechnology in many fields of our society, ranging from healthcare to homeland security and environmental protection. However, enabling the communication in WNSNs is still an unsolved challenge. We acknowledge that there is still a long way to go before having autonomous nanosensors, but we believe that hardware-oriented research and communication-focused investigations will benefit from being conducted in parallel from an early stage. In this paper, we developed energy and spectrum-aware MAC protocols for WNSNs with the objective to achieve fair, throughput and lifetime optimal channel access by jointly optimizing the energy harvesting and consumption processes. To-

wards this end, an important system design parameter, namely, the critical packet transmission ratio (CTR) has been derived, which is the maximum allowable ratio between the transmission time and the energy harvesting time, below which the nanosensor node can harvest more energy than the consumed one, thus achieving perpetual data transmission. Based on the CTR, first, a novel symbol-compression scheduling algorithm, built on the recently proposed pulse-based physical layer technique, is introduced. The symbol-compression solution utilizes the unique elasticity of the inter-symbol spacing of the pulse-based physical layer to allow multiple nanosensors to transmit their packets in parallel without inducing any transmission collisions. In addition, a packet-level timeline scheduling algorithm, built on a theoretical bandwidth-adaptive capacity-optimal physical layer, is proposed with an objective to achieve the balanced single-user throughput with the infinite network lifetime. In this paper, we have considered that all the nanosensors communicate directly with the nano-controller in one hop. As part of our future work, we will investigate optimal decision algorithms for multi-hop communication and routing in WNSNs.

References

- [1] R. Adomavicius, J. Adamonis, A. Biciunas, A. Krotkus, A. Atrashchenko, V. Evtikhiev, V. Ulin, M. Kaliteevski, R. Abram, Terahertz pulse emission from nanostructured (311) surfaces of GaAs, *Journal of Infrared Millimeter and Terahertz Waves* 33 (2012) 599–604.
- [2] I.F. Akyildiz, J.M. Jornet, Electromagnetic wireless nanosensor networks, *Nano Communication Networks* (Elsevier) Journal 1 (1) (2010) 3–19.
- [3] F. Box, Utilization of atmospheric transmission losses for interference-resistant communications, *IEEE Transactions on Communications* 34 (10) (1986) 1009–1015.
- [4] F. Cottone, H. Vocca, L. Gammaitoni, Nonlinear energy harvesting, *Physical Review Letters* 102 (8) (2009).
- [5] G. Deligeorgis, F. Coccetti, G. Konstantinidis, R. Plana, Radio frequency signal detection by ballistic transport in y-shaped graphene nanoribbons, *Applied Physics Letters* 101 (1) (2012) 013502.
- [6] L. Gammaitoni, I. Neri, H. Vocca, Nonlinear oscillators for vibration energy harvesting, *Applied Physical Letters* 94 (2009).

- [7] C. Hansen, Wigig: multi-gigabit wireless communications in the 60 GHz band, *IEEE Wireless Communications* 18 (6) (2011) 6–7.
- [8] IEEE 802.11ad-2012: Wireless LAN Medium Access Control (MAC) and Physical Layer (PHY) Specifications Amendment 3: Enhancements for Very High Throughput in the 60 GHz Band, in: IEEE Standard for Information Technology, Telecommunications and Information Exchange between Systems Std.
- [9] J.M. Jornet, I.F. Akyildiz, Joint energy harvesting and communication analysis for perpetual wireless nanosensor networks in the terahertz band, *IEEE Transactions on Nanotechnology* 11 (3) (2012) 570–580.
- [10] J.M. Jornet, I.F. Akyildiz, Graphene-based plasmonic nano-antenna for terahertz band communication in nanonetworks to appear in IEEE JSAC, Special Issue on Emerging Technologies for Communications (2013).
- [11] J.M. Jornet, I.F. Akyildiz, Information capacity of pulse-based wireless nanosensor networks, in: Proc. of the 8th Annual IEEE Communications Society Conference on Sensor, Mesh and Ad Hoc Communications and Networks SECON, 2011.
- [12] J.M. Jornet, I.F. Akyildiz, Channel modeling and capacity analysis of electromagnetic wireless nanonetworks in the terahertz band, *IEEE Transactions on Wireless Communications* 10 (10) (2011) 3211–3221.
- [13] J.M. Jornet, J.C. Pujol, J.S. Pareta, Phlame: a physical layer aware mac protocol for electromagnetic nanonetworks in the terahertz band, *Nano Communication Networks* 3 (1) (2012) 74–81.
- [14] W. Knap, M. Dyakonov, D. Coquillat, F. Teppe, N. Dyakonova, J. Lusakowski, K. Karpierz, M. Sakowicz, G. Valusis, D. Seljuta, I. Kasalynas, A. Fatimy, Y. Meziani, T. Otsuji, Field effect transistors for terahertz detection: physics and first imaging applications, *Journal of Infrared Millimeter and Terahertz Waves* 30 (2009) 1319–1337.
- [15] I. Llatser, C. Kremers, A. Cabellos-Aparicio, J.M. Jornet, E. Alarcon, D.N. Chigrin, Graphene-based nano-patch antenna for terahertz radiation, *Photonics and Nanostructures – Fundamentals and Applications* 10 (4) (2012) 353–358.
- [16] M. Moore, A. Enomoto, T. Nakano, Y. Okaie, T. Suda, Non-preemptive fixed priority scheduling of hard real-time periodic tasks, in: Proc. of the 7th International Conference on Computational Science, 2007, pp. 881–888.
- [17] T. Otsuji, S. Boubanga Tombet, A. Satou, M. Ryzhii, V. Ryzhii, Terahertz-wave generation using graphene – toward new types of terahertz lasers, *IEEE Journal of Selected Topics in Quantum Electronics* 19 (1) (2013) 8400209.
- [18] R. Piesiewicz, T. Kleine-Ostmann, N. Krumbholz, D. Mittleman, m. Koch, J. Schoebel, T. Kurner, Short-range ultra-broadband terahertz communications: concepts and perspectives, *IEEE Antennas and Propagation Magazine* 49 (6) (2007) 24–39.
- [19] L.A. Ponomarenko, F. Schedin, M.I. Katsnelson, R. Yang, E.W. Hill, K.S. Novoselov, A.K. Geim, Chaotic Dirac billiard in graphene quantum dots, *Science* 320 (5874) (2008) 356–358.
- [20] V. Ryzhii, M. Ryzhii, V. Mitin, T. Otsuji, Toward the creation of terahertz graphene injection laser, *Journal of Applied Physics* 110 (9) (2011) 094503.
- [21] B. Sensale-Rodriguez, R. Yan, M.M. Kelly, T. Fang, K. Tahy, W.S. Hwang, D. Jena, L. Liu, H.G. Xing, Broadband graphene terahertz modulators enabled by intraband transitions, *Nature Communications* 3 (2012) 780+.
- [22] N. Tadayon, S. Khoshroo, E. Askari, H. Wang, H. Michel, Power management in SMAC-based energy-harvesting wireless sensor networks using queuing analysis, *Journal of Network and Computer Applications* 36 (3) (2013) 1008–1017.
- [23] M. Tamagnone, J.S. Gomez-Diaz, J.R. Mosig, J. Perruisseau-Carrier, Reconfigurable terahertz plasmonic antenna concept using a graphene stack, *Applied Physics Letters* 101 (21) (2012) 214102.
- [24] T. Tandai, R. Matsuo, T. Tomizawa, H. Kasami, T. Kobayashi, Mac efficiency enhancement with prioritized access opportunity exchange protocol for 60 GHz short-range one-to-one communications, in: IEEE 73rd Vehicular Technology Conference (VTC), 2011, pp. 1–5.
- [25] L. Vicarelli, M.S. Vitiello, D. Coquillat, A. Lombardo, A.C. Ferrari, W. Knap, M. Polini, V. Pellegrini, A. Tredicucci, Graphene field-effect transistors as room-temperature terahertz detectors, *Nature Materials* 11 (2012) 865–871.
- [26] M.S. Vitiello, D. Coquillat, L. Viti, D. Ercolani, F. Teppe, A. Pitanti, F. Beltram, L. Sorba, W. Knap, A. Tredicucci, Room-temperature terahertz detectors based on semiconductor nanowire field-effect transistors, *Nano Letters* 12 (1) (2012) 96–101.
- [27] Z.L. Wang, Towards self-powered nanosystems: from nanogenerators to nanopiezotronics, *Advanced Functional Materials* 18 (22) (2008) 3553–3567.

- [28] H. Yoo, M. Shim, D. Kim, Dynamic duty-cycle scheduling schemes for energy-harvesting wireless sensor networks, *IEEE Communications Letters* 16 (2) (2012) 202–204.



Pu Wang received the B.S. degree in Electrical Engineering from the Beijing Institute of Technology, Beijing, China, in 2003 and the M.Eng. degree in Computer Engineering from the Memorial University of Newfoundland, St. Johns, NL, Canada, in 2008. He received the Ph.D. degree in Electrical and Computer Engineering from the Georgia Institute of Technology, Atlanta, GA, in 2013. He is currently an Assistant Professor with the Department of Electrical Engineering and Computer Science, Wichita State University, Wichita, KS. He was named BWN Lab Researcher of the Year 2012, Georgia Institute of Technology. He received the TPC top ranked paper award of IEEE DySPAN 2011. He was also named Fellow of the School of Graduate Studies, 2008, Memorial University of Newfoundland. He is a member of IEEE. His research interests include wireless sensor networks, cognitive radio networks, nanonetworks, multimedia communications, wireless communications in challenged environment, Internet of things, and cyber-physical systems.



Jospe Miquel Jornet received the Engineering Degree in Telecommunication and the Master of Science in Information and Communication Technologies from the Universitat Politcnica de Catalunya, Barcelona, Spain, in 2008. He received the Ph.D. degree in Electrical and Computer Engineering from the Georgia Institute of Technology, Atlanta, GA, in 2013, with a fellowship from “la Caixa” (2009–2010) and Fundacin Caja Madrid (2011–2012). He is currently an Assistant Professor with the Department of Electrical Engineering at the University at Buffalo, The State University of New York. From September 2007 to December 2008, he was a visiting researcher at the Massachusetts Institute of Technology, Cambridge, under the MIT Sea Grant program. He was the recipient of the Oscar P. Cleaver Award for outstanding graduate students in the School of Electrical and Computer Engineering, at the Georgia Institute of Technology in 2009. He also received the Broadband Wireless Networking Lab Researcher of the Year Award at Georgia Institute of Technology in 2010. He is a member of the IEEE and the ACM. His current research interests are in electromagnetic nanonetworks, graphene-enabled wireless communication, Terahertz Band communication networks and the Internet of Nano-Things.



M.G. Abbas Malik received the Ph.D. in Computer Science degree from University of Grenoble I, France and Master in Computational Linguistics from University of Paris 7 – Denis Diderot, France in 2010 and 2006 respectively. He also received the Mater in Computer Science degree from Punjab University College of Information Technology, University of the Punjab, Pakistan in 2003. He served as Assistant Professor in COMSATS Institute of Information Technology Lahore, Pakistan for academic year 2010–2011. Since September 2011, he has been working as Assistant Professor in Faculty of Computing and Information Technology, King Abdulaziz University, Jeddah, Saudi Arabia.

Nadine Akkari received the B.S and the M.S. degrees in Computer Engineering from University of Balamand, Lebanon, in 1997 and 1999, respectively. She received the Master degree in Networks of Telecommunications from Saint Joseph University and the Faculty of Engineering of the Lebanese University, Lebanon, in 2001 and Ph.D. degree in Networking from National Superior School of Telecommunications (ENST),

France, in 2006. She is currently an assistant professor with the faculty of Computing and Information Technology at King Abdulaziz University, Jeddah, Saudi Arabia. She is a member of IEEE. Her research interests are in wireless networks, mobility management protocols, and nanonetworks.



Ian F. Akyildiz received the B.S., M.S., and Ph.D. degrees in Computer Engineering from the University of Erlangen-Nrnberg, Germany, in 1978, 1981 and 1984, respectively. Currently, he is the Ken Byers Chair Professor in Telecommunications with the School of Electrical and Computer Engineering, Georgia Institute of Technology, Atlanta, the Director of the Broadband Wireless Networking (BWN) Laboratory and the Chair of the Telecommunication Group at Georgia Tech. Since 2013, he is a FiDiPro Professor (Finland Distinguished

Professor Program (FiDiPro) supported by the Academy of Finland) in the Department of Electronics and Communications Engineering, at Tampere

University of Technology, Finland, and the founding director of NCC (Nano Communications Center). Since 2011, he is a Consulting Chair Professor at the Department of Information Technology, King Abdulaziz University (KAU) in Jeddah, Saudi Arabia. Since 2008, he is also an honorary professor with the School of Electrical Engineering at Universitat Politcnica de Catalunya (UPC) in Barcelona, Catalunya, Spain and the founding director of N3Cat (NaNoNetworking Center in Catalunya). He is the Editor-in-Chief of Computer Networks (Elsevier) Journal, and the founding Editor-in-Chief of the Ad Hoc Networks (Elsevier) Journal, the Physical Communication (Elsevier) Journal and the Nano Communication Networks (Elsevier) Journal. He is an IEEE Fellow (1996) and an ACM Fellow (1997). He received numerous awards from IEEE and ACM. His current research interests are in nanonetworks, Long Term Evolution Advanced (LTE-A) networks, cognitive radio networks and wireless sensor networks.